International Journal of Hydrological and Environmental for Sustainability
Volume 1, Issue 3, 132-145
e_ISSN: 2828-5050
https://www.journal.foundae.com/index.php/ijhes

Magnetic Properties Analysis of Synthesis of Poly-(Vinyl Alcohol)/Clay/Nanomagnetite Composites: Application for Wastewater Filter

Benny Wahyudianto*
Department of Chemistry,
Osaka University,
JAPAN

Langit Cahya Adi
Department of Chemistry,
Osaka University,
JAPAN

***Correspondence: E-mail:** wahyudiantob17@chem.sci.osaka-u.ac.jp

Article Info

Article history:

Received: September 20, 2022
Revised: October 25, 2022
Accepted: October 31, 2022

Abstract

The composites of poly–(vinyl alcohol) (PVA)/clay/Fe_3O_4 (magnetite) were synthesized with Fe(II) in-situ via hydrolysis method. The films were obtained as films by employing natural clay containing montmorrilonite (aluminosilicate) using casting technique. The weight variations of each component were also investigated. The resulting films were characterized with fourier transform infrared (FT-IR) to analyze their functional groups, and then X-ray diffractometer (XRD) was used to check the formation of magnetite and it was combined with Deybe-Scherrer equation to determine the theoretical size of magnetite. Along with that, vibrating sample magnetometer (VSM) analysis was carried out in order to measure the magnetic saturation brought by the magnetite inside composite system. FT-IR spectra showed peak around 610 $cm^{-1}$and XRD diffracttogram pattern showed four characteristic peaks indicating (200); (311); and (511). Both results confirmed the formation of magnetite inside composite system. The result of VSM measurement showed that increasing PVA weight would lead into the decrease of the magnetic saturation of magnetite-contained composites due to hydroxyl group from PVA control its crystalline. Conversely, the reverse plot would be acquired if the precursor Fe(II)weight was augmented in the composite system due to another iron oxide species i.e.: goethite was predicted to form as the intermediate of magnetite. On the other hand, the amount variation of the aluminosilicate material was resulting no coherent plot through magnetic saturation value.

Keywords: poly–(vinyl alcohol); clay; magnetite; magnetism; composite; wasterwater

To cite this article: Wahyudianto, B. and Adi, L. C. (2022). Magnetic Properties Analysis of Synthesis of Poly-(Vinyl Alcohol)/Clay/Nanomagnetite Composites: Application for Wastewater Filter. *International Journal of Hydrological and Environmental for Sustainability, 1*(3), 132-145. https://doi.org/10.58524/ijhes.v1i3.145

INTRODUCTION

Composite materials employing magnetic property may be applied in many applications, one of them is as an absorbent for waste water (Bronzino, J, D., 2014). In nanometer range, materials possessing magnetic character can create unique magnetization properties that further can present magnetic properties if they are incorporated into another substances into composites (Sabara et al., 2022a).

One factor of a particular magnetic property in the sense of magnetization comes from the existence of an atom with unpaired electron in its configuration, many of which were d-block transition elements (Sabara et al., 2022b) and f-block lanthanide metal (Seol et al., 2004). Iron is one of famous transition metal which is often used due to its relatively high abundance in nature (Shimoiizaka, J., 1996). Iron has several example of magnetic oxide compounds such as magnetite (Fe_3O_4), hematite (α–Fe_2O_3), maghemite (γ–Fe_2O_3) and geothite (γ–FeOOH); and the most profound

magnetic one is magnetite (Simon M. D and Geim A. K., 2000). Magnetite has an appearance of a black precipitate and is affected to external magnetic field. Magnetite could be synthesized though several methods, such as hydrothermal; micro-emulsion; solvothermal; co-precipitation, and hydrolysis (Sinha et al., 2004). In case of hydrolysis method, magnetite could be prepared from single precursor Fe(II) or double precursor (known as co-precipitation) Fe(II) and (III).However, single precursor technique would produce higher size and magnetic property compared to the co-precipitation one, yet the oxide material can be produced in nanometer scale by both techniques (Sorensen C. M. and Klabunde K. J., 1998). Further, magnetite can be formed if the ratio of Fe(II)/Fe(III) reaches 1/2 and in particular, Fe(II) is more likely to be oxidized becoming Fe(III) under air atmosphere hence single precursor method in gaining magnetite needs a stabilizer. Some natural and synthetic polymers were promising substances to become stabilizer at single pot reaction, like chitosan; alginate; poly–(ethylene glycol); and poly–(vinyl alcohol) or PVA (Stevens et al., 2008). In case of PVA; it consists of hydroxyl group as side chain. Then, PVA can be soluble in neutral pH at moderate temperature. The hydroxyl groups of the backbones are able to interact via hydrogen bond creating pores which is in advance filled by water molecules. The pristine PVA character can be modified based on host material. In case of PVA and magnetite composite, this composite had been synthesized before (Yang F, Wolke J G C and Jansen J A., 2008). According to each property, it has big change that PVA can stabilize the formation of magnetite from the beginning by reason of the formation of magnetite can happen in PVA solution. After magnetite is formed, it could not be dissolved any longer in water solvent and later would precipitate spontaneously. After that, the magnetite dispersion inside the composite may decrease. Magnetite may agglomerate inside because it has reactive surface towards oxygen atoms. In another reference, clay was used to adsorb organic dyes and decrease the possibility to agglomerate again via cationic exchange onto the surface (Stock U. A. and Vacanti J. P. 2001).

Natural clay is a combination from many sources, such as montmorillonite, vercutile, illite, and quartz; which is the novelty brought by this report. In case of quartz, it was an impurity and it had siloxane bond (Si–O–Si). Basic treatment to natural clay would change siloxane bond into silicate ion and separate it with washing treatment. On the other hand, basic treatment would increase the active site of aluminosilicate functional group by possessing negative ions (Sun et al., 1998). When clays have more negative site, the number of cation can increase to balance the charge. Then the counter ion can change with positive site of magnetite via cation exchange. This is one way to prevent further agglomeration reaction among magnetite.

In this paper, we report the synthesis of PVA-clay-magnetite composite using hydrolysis method with one-pot synthesis technique. Magnetite was synthesized using single precursor Fe(II). The aim of this investigation is to study about the effect of PVA/clay/Fe(II)-precursor weight variations to magnetic property.

METHOD

Basic treatment of natural clay

About 10 g of 400 meshes natural clay refluxed with 50 mL of 2.0 M NaOH for approximately 8 h at 100 °C. Basic treatment clay washed with 50 mL of NaOH 1.0 M and distilled water until constant pH. Then the base-treated clay was filtered with Whattman 41 filter paper and heated overnight at 100 °C.

Synthesis Fe_3O_4 in composite film

PVA with weight variation of 1.5; 2.0; 2.5; 3.0; or 3.5 g were dissolved in 50 mL of distilled water at 60 °C until a homogenous solution was obtained. The PVA solution was added to the suspension of 0.05 g of base-treated clay in 10 mL of distilled water. In a separate beaker, a 0.28 g $FeSO_4 \cdot 7H_2O$ was dissolved in 10 mL of distilled water, and consecutively added with 0.5 M NaOH 10 mL. The solution was added to the PVA-basic treatment clay mixture. The resulting suspension was subsequently evaporated at 80 °C until the total volume of 20-30 mL. When the total volume had been reached, the mixture was casted into a 9.6 cm diameter of petri dish, and then cooled for 3 days at room temperature.

Magnetic characterization

All samples were weighed by XND GR-200 measurement scale. It was tested by providing an external magnetic field by Vibrating Sample Magnetometer (VSM) OXFORD VSM1.2H with magnetization ranging -1 to 1 T.

Table 1. Variation of composite

Variation	Weight (gram)		Amount of Fe(H) (mmol)
	PVA	Montmorrilonite	
PVA	1.50	0.5	1.00
PVA	2.00	0.5	1.00
PVA	2.50	0.5	1.00
PVA	3.00	0.5	1.00
PVA	3.50	0.5	1.00
Montmorrilonite	2.50	0.00	1.00
Montmorrilonite	2.50	0.01	1.00
Montmorrilonite	2.50	0.15	1.00
Montmorrilonite	2.50	0.20	1.00
Fe (II)	2.50	0.5	0.32
Fe (II)	2.50	0.5	0.50
Fe (II)	2.50	0.5	1.00
Fe (II)	2.50	0.5	1.26
Fe (II)	2.50	0.5	1.50

(**Source :** Data of this study)

RESULTS AND DISCUSSION

Matrix dependent

Structural analysis by FT-IR spectroscopy and XRD

The formation of magnetite had successfully synthesized inside PVA network and was considered to be in-situ formation mechanism. PVA in **Figure 1(a)** shows 2 peaks around 1635 and 3448 cm^{-1}, indicating trapped water molecule within the samples (Tang et al., 2004). The absence of C–O bond is a sign that PVA is fully hydrolyzed from its initial monomer, poly–(vinyl acetate), around 1760-1690 cm^{-1}. Fe–O bond appears at around 586 cm^{-1} but this peak is shifted into 617 cm^{-1} inside composite system in **Figure 1(c)-(h)**.The peaks of Fe–O bonds decrease gradually starting from PVA 1.50 to 3.50 correspond to the presence of magnetite encapsulate inside composite and it cannot be detected with detector.

The XRD analysis was used to examine the crystalline of each material and to make sure the formation of magnetite inside composite system. Diffractogram of PVA in **Figure 2(a)** shows one highest peak around $2\theta = 19.7°$ and it indicates that PVA has semi-crystalline structure. Crystalline region may come from the ordered phases of PVA. According to the diffractogram data of clay in **Figure 2(b)**, basic treatment clay gave montmorillonite as the major composition, and then a trace amount of illite and quartz but the peaks look like amorphous compared to the other diffractograms. The characteristic peaks of them cannot be well detected in **Figure 2(b)** due to the relatively small intensity compared to the others (Yoon D M and Fisher J P., 2006; Yashimoto et al., 2003; Yoshizawa S., Fourmy D. and Puglisi J. D. 1998; Zaitsev et al., 1999). In case of magnetite formation, magnetite peak from standard and composite variations were compared. The result showed several similar characteristic peaks around $2\theta = 31.37$; 34.78; and 56.45°. The peaks above are well matched to magnetite peak in JCPDS No. 86-1354 and reflected lattice planes with Miller indexes in sequence (200); (311); and (511) (Weissleder et al., 1995).

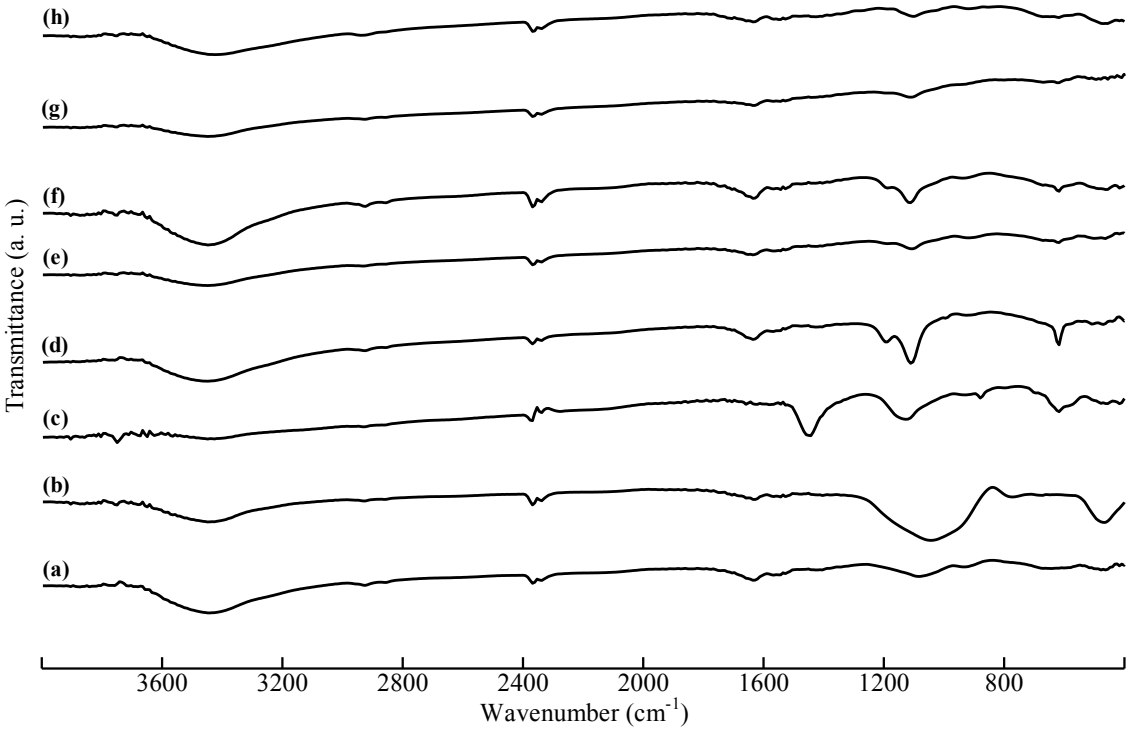

Figure 1. Infrared spectra of PVA dependent of composite: (a) PVA film; (b) PVA-clay composite film; (c) magnetite (standard); PVA weight variation (d) 1.5; (e) 2.0; (f) 2.5; (g) 3.0; and (h) 3.5 gram cm.

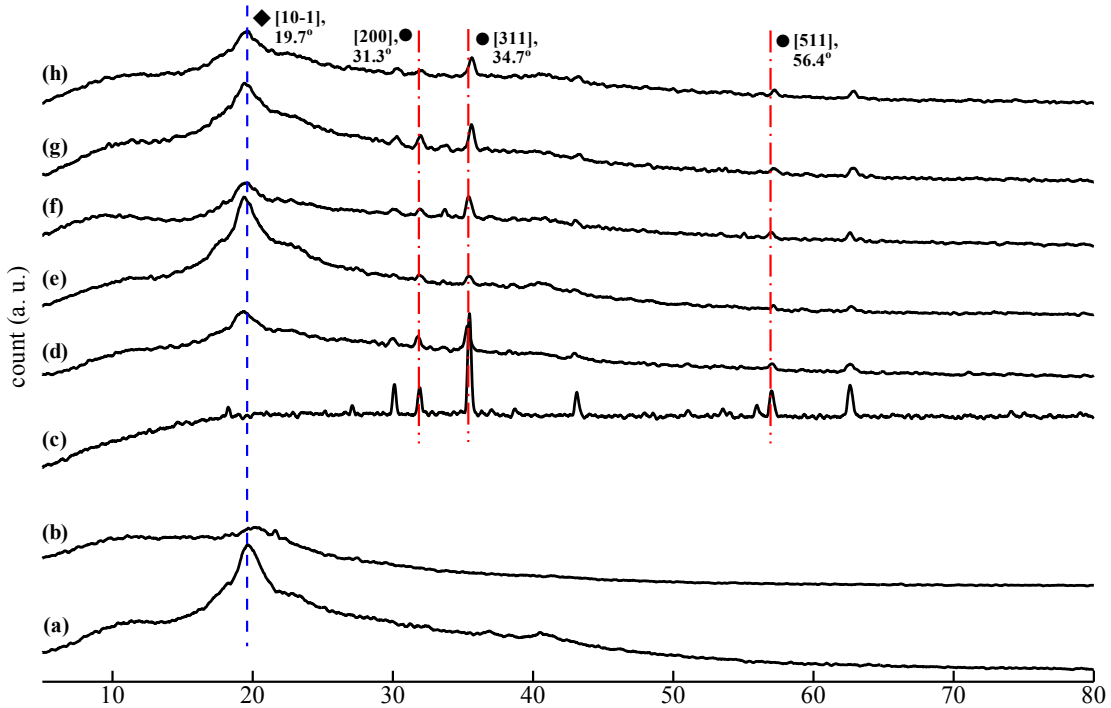

Figure 2. Diffractogram of PVA dependent of composite: (a) PVA film; (b) PVA-clay composite film; (c) magnetite (standard); PVA weight variation (d) 1.5; (e) 2.0; (f) 2.5; (g) 3.0; and (h) 3.5 gram.

Table 2. Size of magnetite (calculated by Deybe-Scherrer equation) for matrix dependent.

Variation of PVA weight (g)	Size of magnetite (nm)
1.5	21.7
2.0	15.8

2.5	17.2
3.0	19.8
3.5	16.5

(**Source :** Data of this study)

From the diffractogram results, the size of magnetite and crystalline region can be determined to get intermediate information to explain its magnetic property. The size of magnetite can be measured by Debye-Scherrer equation, $D = \frac{k\,\lambda}{B\cos\theta}$. According to the equation, where D is the crystal size; k is crystal roundness constant and generally expressed by 0.9; B represents Full Width at High Maximum (FWHM) of analyzed peak at θ. In case of magnetite, the size can be analyzed at 2θ around 34° (311). **Table 2** shows magnetite size in nanometer range. Unfortunately, Deybe-Scherrer result only represents theoretical magnetite size in small area (Zambaux M F, Bonneaux F and Gref F., 1998; Zhang J and Misra R D K., 2007). Because of that, the size particle from the calculation cannot express the average value of the entire magnetite size.

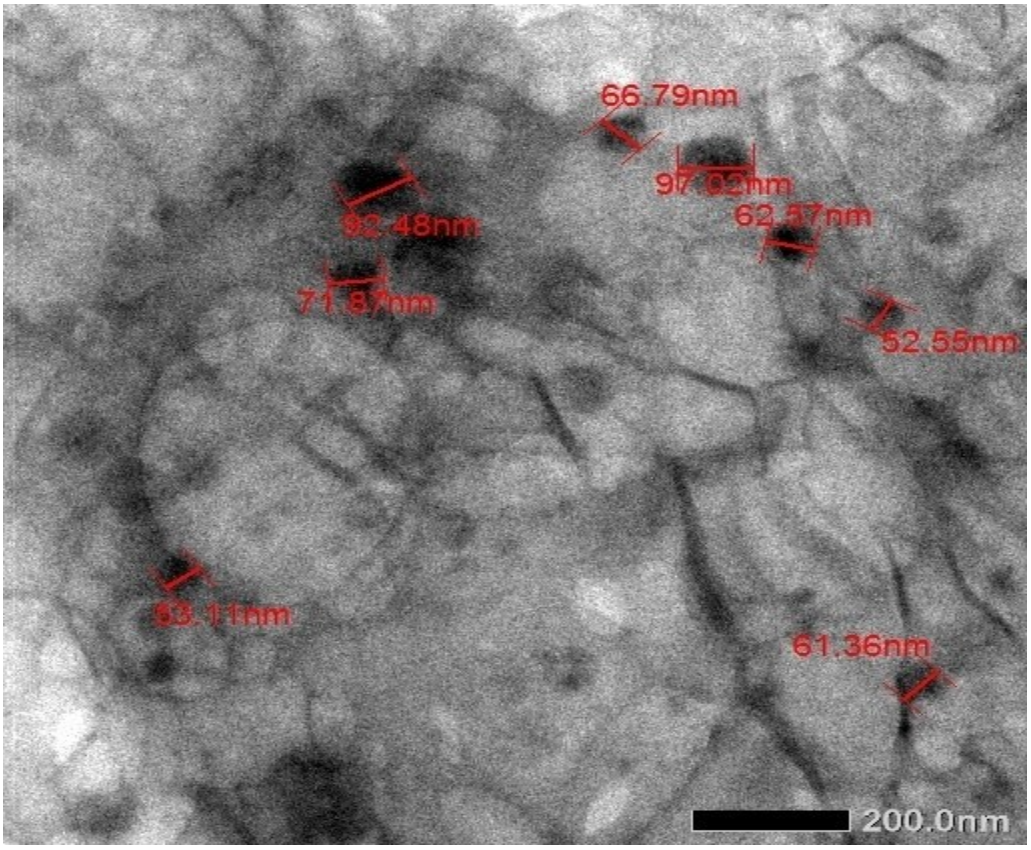

Figure 3. Micrograph of PVA 2.5. 8cm

Then, transmission electron microscopy (TEM) micrograph from PVA weight variation (PVA 2.5) can confirm that the size of magnetite is in nanometer range in **Figure 3**. The micrograph showed magnetite was not homogenous size and it indicated that magnetite agglomerated to form larger size.

Table 3. Crystalline and amorphous area of magnetite

Variation of PVA weight (g)	**Area (%)**	
	Crystalline	**Amorphous**
1.5	31.61	68.39
2.0	16.55	83.45
2.5	19.55	80.45
3.0	20.44	79.55
3.5	30.67	69.33

(**Source :** Data of this study)

To define the crystalline region, we calculated the result from the intensity of three characteristic peaks from the magnetite and multiplied by the FWHM from each peak. Then, the result of each composite was divided by the standard value (Zhang Y, Kohler N and Zhang M., 2002; Zhao et al., 2001). According **Table 3**, the crystalline region of PVA dependent in composite would increase if the weight of matrix increases (except PVA 1.5). In this phenomenon, we assumed that Fe(II) cannot move fast if the density of PVA increases in solution. The highest PVA weight in composite would affect to slow formation of magnetite to reach Fe(II)/Fe(III) 1/2. In that time, the arrangement of magnetite more organized.

Magnetization analysis in matrix dependent

On the other hand, magnetic property represented by B-H loop showed **Figure 4** that the magnetization was decreased when the PVA weights were increased.

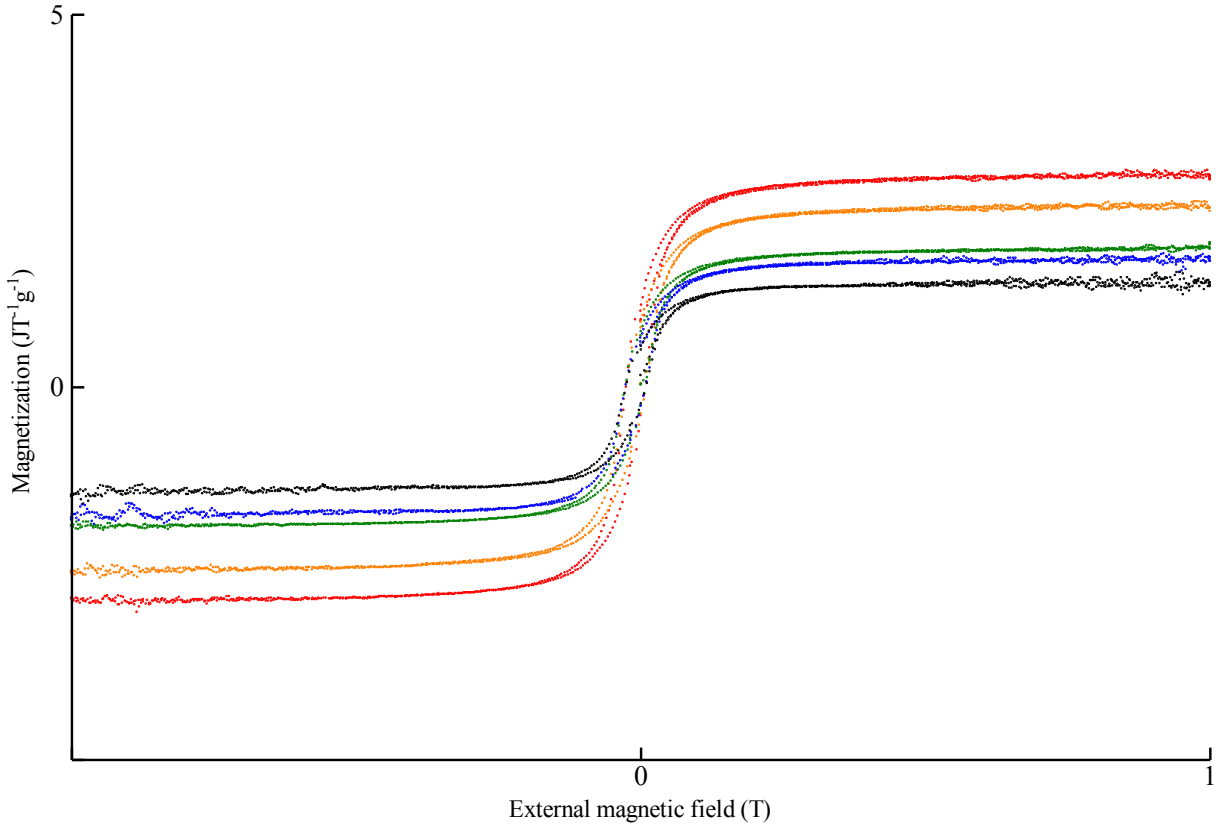

Figure 4. Hysteresis loop of PVA dependent in composite: (red) 1.5; (yellow) 2.0; (green) 2.5; (blue) 3.0; and (black) 3.5 gram.

Another investigation showed the correlation among magnetic property, precursor, and size; and then higher particle size contributed to higher magneticity (Weissleder et al., 2000). During this investigation, higher crystalline region affected to higher magnetic field due to high crystalline region means the iron can arrange the structure well with opposite unpairing electron inside magnetite structure.

Dependence on the filler

Structural analysis by FT-IR spectroscopy and XRD

The dependence of the iron oxide formation is theoretically expected due to the possible interaction via hydrogen bonding between the aluminosilicate materials with the organic matrix polymer by their corresponding functional groups. In the previous publication (Williams et al., 2005), the presence of aluminosilicate can assist the dispersion of magnetite as the clay is a dispersion agent. Hence, it can be predicted that there will be changes or alteration of magnetite crystal structure which further may lead into its different magnetic properties.

In this given variation, the amount of PVA was set to be 2.5 g. The first analysis was taken out for the FT-IR spectrometry with the wavelength range 400-4000 cm^{-1} but the focus in this section will be on the vibrational absorption on the range 400-1250 cm^{-1}. The spectra of the composites are shown on **Figure 5** above.

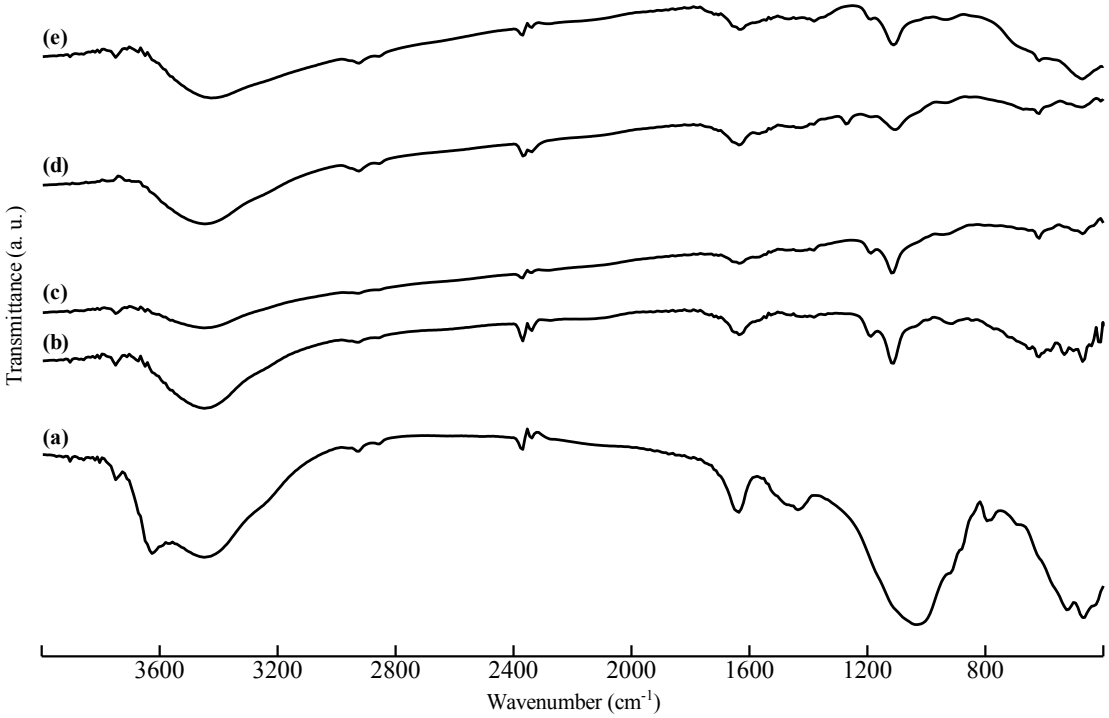

Figure 5. Infrared spectra of clay dependent of composite: (a) 0.00; (b) 0.01; (c) 0.15; and (d) 0.20 gram

According to the spectra, there is a pronounced peak at around 617 cm^{-1} which is indicating the presence of Fe–O vibration. The similar absorption was also found by previous scientist (Woo et al., 2004). Even so, the FT-IR spectrophotometer cannot detect and cannot analyze the influence of the filler to magnetite formation. Therefore, another analysis by XRD was done to as a complementary.

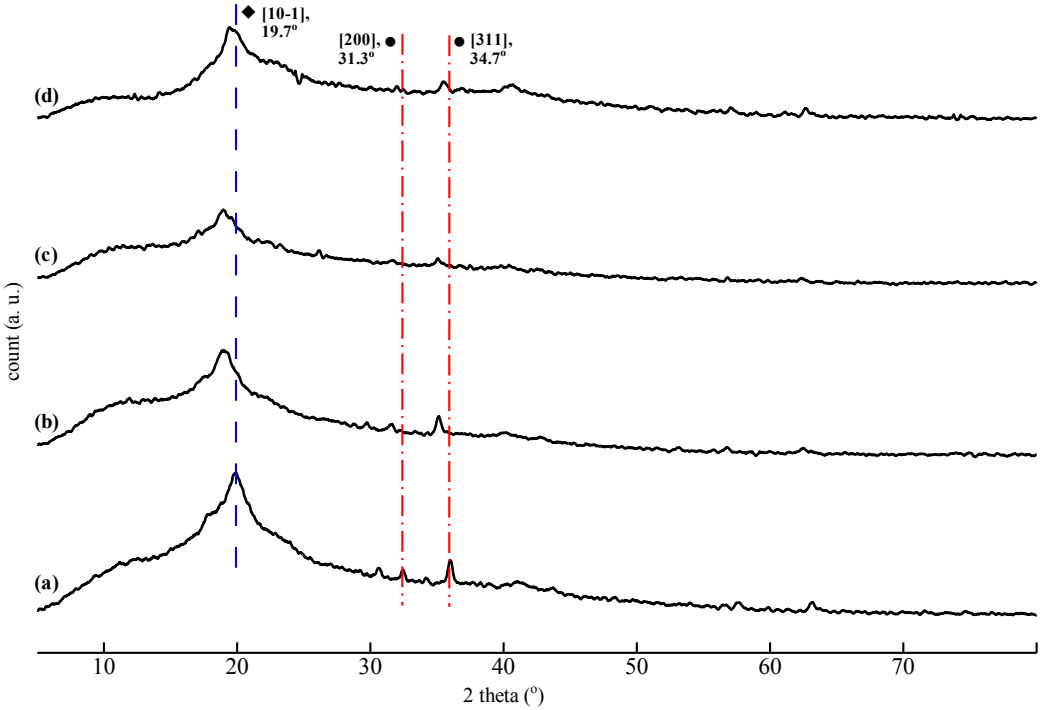

Figure 6. Diffractogram of clay dependent of composite: (a) 0.00; (b) 0.01; (c) 0.15; and (d) 0.20 gram

According to the diffractogram of the composites on **Figure 6**, the characteristic peak of PVA matrix was relatively dominant compared to the other peaks in each composite. However, the characteristic peaks of magnetite were not obviously observed, and this phenomenon could be inferred as an indication that magnetite were not well formed particularly in the term of crystallinity. According to Yamaguchi et al., (2005), the addition of additive into PVA can affect the crystal formation of magnetite inside the polymer material (Xiong et al., 2001). It must also be stated that the presence of clay inside the composite did not cause any distinct magnetite particle size in each composite film and therefore the saturated magnetization on the next explanation did not depend on the amount-varied clay either.

Table 4. Size of magnetite (calculated by Deybe-Scherrer equation) for filler dependent

Variation of montmorrilonite (gram)	Size of Fe_3O_4 (nm)
0.00	21.3
0.01	20.6
0.15	25.1
0.20	15.4

(**Source :** Data of this study)

Magnetization analysis in clay dependent

Based on B-H curve in **Figure 7**, clay variation did not give any clear evidence to magnetic properties, due to the agglomeration process happening among the clay.

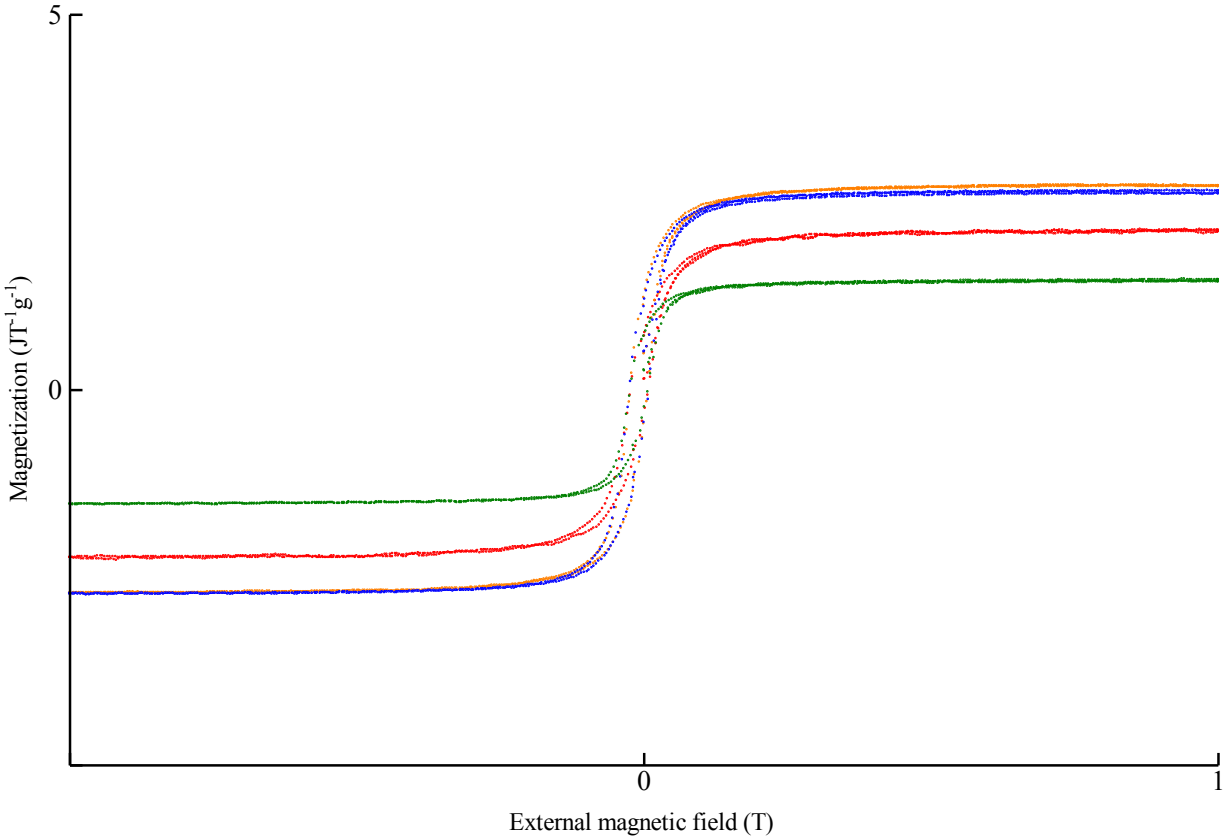

Figure 7. Hysteresis loop of clay dependent in composite: (red) 0.00; (yellow) 0.01; (green) 0.15; and (blue) 0.20 gram

Dependence on the precursor/Fe(II)

Structural analysis by FT-IR spectroscopy and XRD

In case of precursor variation, we assumed that more precursors will increase the magnetic saturation. Then, we wanted to investigate the phenomena during the increasing of precursor weight. In **Figure 8**, the presence of Fe–O bond can be detected at around 617 cm^{-1}. Increasing precursor weight should increase magnetite in the composite. In contrast, infrared spectra detected a lower peak when the amount of precursor was increased. According to reaction 2.3, formation of magnetite would produce water as a byproduct. According to Yin et al., (2003), the formation of goethite and magnetite are shown below:

$$Fe^{2+} + 2OH^- \rightarrow Fe(OH)_2 \quad (2.1)$$

$$4Fe(OH)_2 + O_2 \rightarrow 4\alpha\text{–}FeOOH + 2H_2O \quad (2.2)$$

$$2\alpha\text{-}FeOOH + Fe^{2+} + 2OH^- \rightarrow Fe_3O_4 + 2H_2O \quad (2.3)$$

On contrary, the peak of O–H(stretching) at around 3440 cm^{-1} showed an increased transmittance. It indicated that the number of O-H (stretching) was decreased along with the increasing weight of precursor. This evidence showed that this peak could be arising from $Fe(OH)_2$ or goethite, and then it would decrease gradually due to the formation of magnetite from **Figure 8(a) to (e)**.

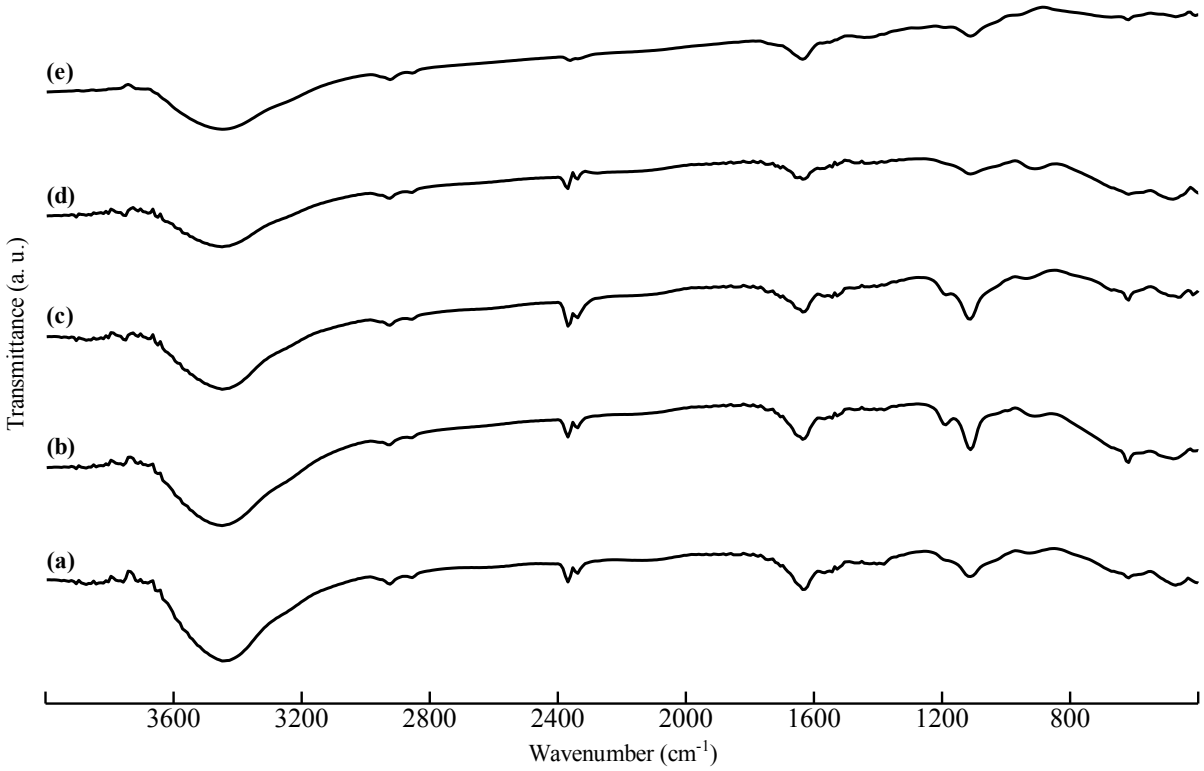

Figure 8. Infared spectra of Fe(II) dependent: (a) 0.32; (b) 0.50; (c) 1.00; (d) 1.26; and (e) 1.50 mmol.

Sump Dimension Recommendation

The presence of S=O (stretching) shown at peak around 1111 cm^{-1} and the intensity decreased while the weight of precursor increased. The reason can be rationalized based on the previous chemical reaction (2.1) to (2.3).[23] The increased precursor reaching to excess amount did not accompanied with the addition of any base in the solution. Hence, water molecules as final product might be protonated, resulting to a base and an acid in the same time. The base species would be used for magnetite formation and acid would react further with sulphate ion (anionic from salt precursor) to become HSO_4^-. This phenomenon is one of the factors of decreasing S=O (stretching) from **Figure 8(a) to (e)**.

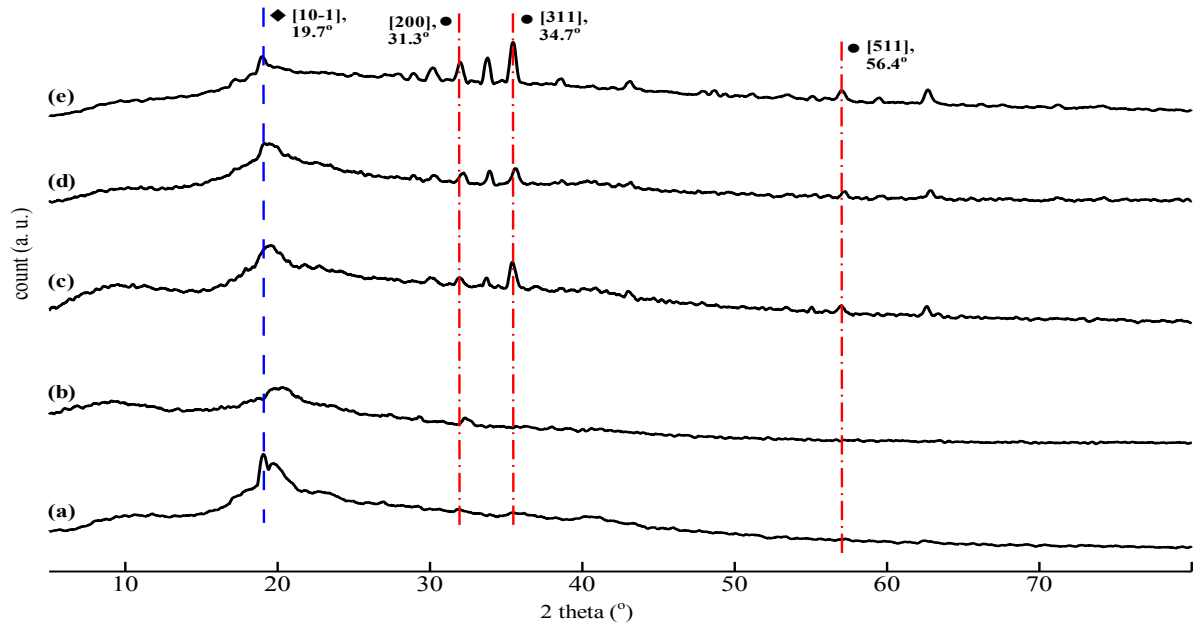

Figure 9. Diffractogram of Fe(II) dependent: (a) 0.32; (b) 0.50; (c) 1.00; (d) 1.26; and (e) 1.50 mmol

In **Figure 9**, three highest peaks of magnetite only appeared with addition of precursor greater than or equal to 1 mmol, but all composites showed magnetic properties. This phenomenon emphasized that goethite was formed in as an intermediate compound of magnetite. Regarding about **Figure 9(a)** and **Figure 9(b)**, magnetite was not synthesized below 1 mmol of precursor in the composites. In fact, the characteristic peaks of magnetite were absent. According to the Deybe-Scherrer equation, the size of magnetite was below 20 nm which shown in **Table 5**.

Table 5. Size of magnetite (calculated by Deybe-Scherrer equation) for filler dependent

Variation of FE(II) (mmol)	Size of Fe_3O_4 (nm)
0.32	-
0.50	-
1.00	17.2
1.26	17.5
1.50	18.5

(**Source :** Data of this study)

Magnetization analysis in precursor dependent

In **Figure 10**, B-H curves of precursor dependent showed two groups. The first one is goethite based (the red and yellow lines) and the other is magnetite base (green, blue, and black lines). This result was reflected by both infrared spectra and diffractogram data. Moreover, it can confirm that the magnetization of magnetite is bigger than that of goethite. When the mole ratio of the precursor increased, the possibility of magnetite formation and the magnetization value would also increase.

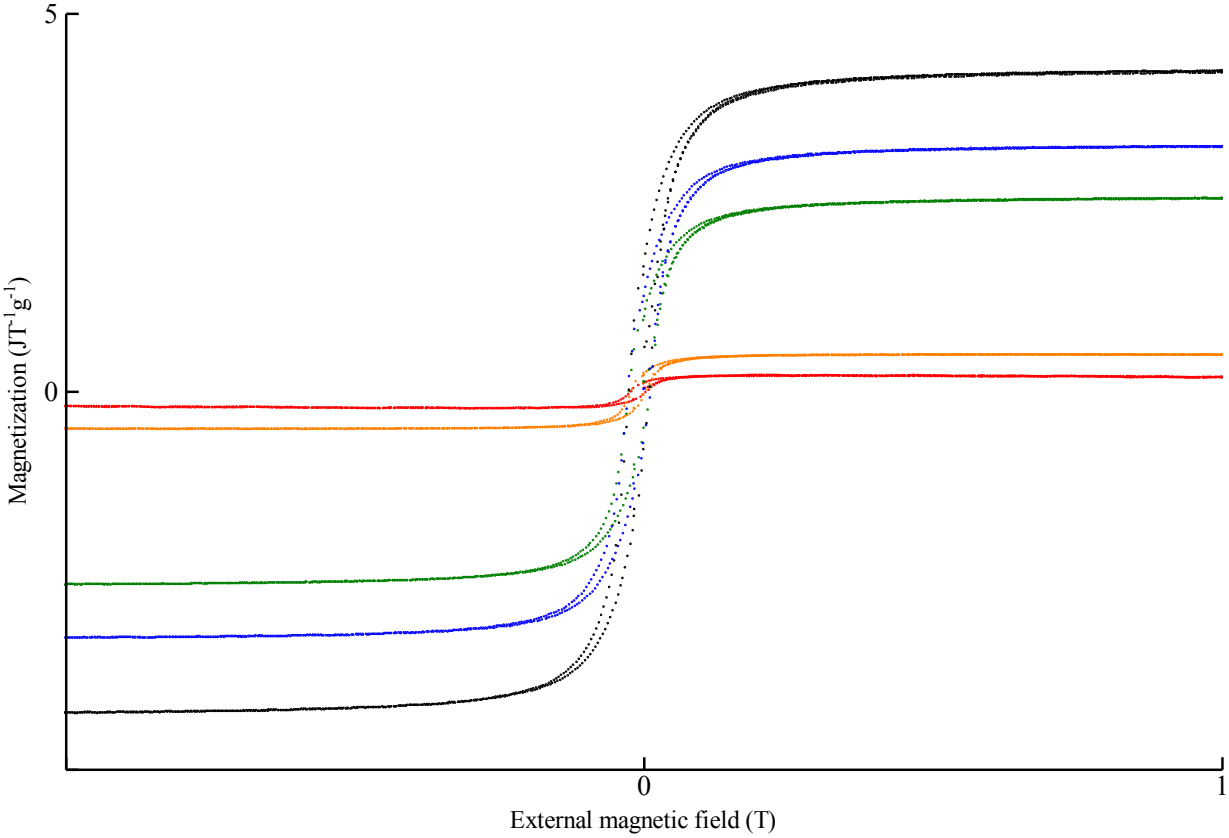

Figure 10. Hysteresis loop of Fe(II) dependent: (a) 0.32; (b) 0.50; (c) 1.00; (d) 1.26; and (e) 1.50 mmol

The result of magnetic properties analysis provides information that the synthesis of poly-(vinyl alcohol)/clay/nanomagnetite composites can be used as a water filter tool, because its magnetic properties can absorb metal levels contained in wastewater or other water.

CONCLUSION

The characteristic peak of PVA matrix was relatively dominant compared to the other peaks in each composite. However, the characteristic peaks of magnetite were not obviously observed, and this phenomenon could be inferred as an indication that magnetite were not well formed particularly in the term of crystallinity. In case of precursor variation, we assumed that more precursors will increase the magnetic saturation. Then, we wanted to investigate the phenomena during the increasing of precursor weight. The presence of Fe–O bond can be detected at around 617 cm^{-1}. Increasing precursor weight should increase magnetite in the composite. In contrast, infrared spectra detected a lower peak when the amount of precursor was increased.the peak of O–H(stretching) at around 3440 cm^{-1} showed an increased transmittance. It indicated that the number of O-H (stretching) was decreased along with the increasing weight of precursor. This evidence showed that this peak could be arising from $Fe(OH)_2$ or goethite, and then it would decrease gradually due to the formation of magnetite The presence of S═O (stretching) shown at peak around 1111 cm^{-1} and the intensity decreased while the weight of precursor increased. The increased precursor reaching to excess amount did not accompanied with the addition of any base in the solution. Hence, water molecules as final product might be protonated, resultingto a base and an acid in the same time. The base species would be used for magnetite formation and acid would react further with sulphate ion (anionic from salt precursor) to become HSO^{4-}. This phenomenon is one of the factors of decreasing S═O (stretching). The first one is goethite based (the red and yellow lines) and the other is magnetite base (green, blue, and black lines). This result was reflected by both infrared spectra and diffractogram data. Moreover, it can confirm that the magnetization of magnetite is bigger than that of goethite. When the mole ratio of the precursor increased, the possibility of magnetite formation and the magnetization value would also increase.

ACKNOWLEDGMENT

The authors would like to thank all reviewers who have provided suggestions to improve this article. The authors are grateful to Universitas Gadjah Mada for providing the opportunity to conduct research and provide direction and guidance during the research.

CONFLICTS OF INTEREST

The authors declare no conflict of interest concerning the publication of this article. The authors also confirm that the data and the article are free of plagiarism.

REFERENCES

Joseph D.Bronzino, 2014., Biomedical Engineering Fundamentals, Taylor & Francis Group, pp. 37-1-37-18.

Sabara, Z., Mutmainnah, A., Kalsum, U., Afiah, I, N., Husna, I., Saregar, A., Irzaman, and Umam, R. 2022. “Sugarcane Bagasse as the Source of Nanocrystalline Cellulose for Gelatin-Free Capsule Shell”, *International Journal of Biomaterials*, vol. 2022, Article ID 9889127, 8 pages, 2022. https://doi.org/10.1155/2022/9889127

Sabara, Z.; Anwar, A.; Yani, S.; Prianto, K.; Junaidi, R.; Umam, R.; Prastowo, R. 2022. Activated Carbon and Coconut Coir with the Incorporation of ABR System as Greywater Filter: The Implications for Wastewater Treatment. Sustainability, 14, 1026. https://doi.org/10.3390/su14021026

Seol Y. J., Lee J. Y., Park Y. J., Lee Y. M., Ku Y., Rhyu I. C., Lee S. J., Han S. B. and Chung C. P. 2004, "Chitosan sponges as tissue engineering scaffolds for bone formation", *Biotechnology Letters*, vol. 26, pp.1037-1041.

Shimoiizaka, J. 1966, "Flocculation and dispersion of powders in liquids", Funtai Oyobi Funmatsuyakin (*Japan Soc. Powder and Powder Metallurgy*), vol. 13, pp. 263-274.

Simon M. D. and Geim A. K., 2000, "Diamagnetic levitation: Flying frogs and floating magnets ", *Journal of Applied Physics*, vol. 87, pp. 6200.

Sinha V.R., Bansal K., Kaushik R., Kumria R. and Trehan A. 2004, "Poly-ε-caprolactone microspheres and nanospheres: an overview", *International Journal of Pharmaceutics*, vol. 278, pp. 1-23.

Sorensen C. M. and Klabunde K. J. 1998. Nanoscale materials in chemistry, New York: Wiley.

Stevens, B., Yang, Y., Mohandas, A., Stucker, B. and Nguyen, K. T. 2008, "A Review of Materials, Fabrication Methods, and Strategies Used to Enhance Bone Regeneration in Engineered Bone Tissues", *Journal of biomedical materials research Part B: applied biomaterials*, vol. 85B, pp. 573-582.

Stock U. A. and Vacanti J. P. 2001, "Tissue engineerng: Current State and Prospects", Annu. Rev. Med, vol. 52, pp. 443–51.

Sun Z. X., Su F. W., Forsling W. and Samskog P. O. 1998, "Surface characteristics of magnetite in aqueous suspension", *Journal of colloid and interface science*, vol. 197, pp. 151-159.

Tang Z. G., Black R.A., Curran J. M., Hunt J. A., Phoodes N. P. and Williams D. F. 2004, "Surface properties and biocompatibility of solvent-cast poly[e-caprolactone] films", *Biomaterials*, vol. 25, pp. 4741-4749.

Weissleder R., Bogdanov A., Neuwelt E. A. and Papisov M. 1995, "Long circulation iron oxides for MR imaging", *Adv. Drug Deliv Rev*, vol. 16, pp. 321-334.

Weissleder R., Moore A., Mahmood U., Bhorade R., Benveniste H., Chiocca E. and Basilion J. B. 2000, "In vivo MR imaging of transgene expression", *Nat Med*, vol. 6, pp. 351-355.

Williams J. M., Adewunmi A., Schek R. M., Flanagan C. L., Krebsbach P. H., Feinberg S. E., Hollister S. J. and Das S. 2005, "Bone tissue engineering using polycaprolactone scaffolds fabricated via selective laser sintering", *Biomaterials*, vol. 26, pp. 4817-4827.

Woo K., Hong J. Choi S., Lee H., Ahn J., Kim C. and Lee S. W. 2004, "Easy synthesis and magnetic properties of iron oxide nanoparticles", *Chem. Mater*, vol. 16, pp. 2814-2818.

Xiong Z., Yan Y., Zhang R. and Sun L. 2001, "Fabrication of porous poly(L-lactic acid) scaffolds for bone tissue engineering via precise extrusion", *Scripta Materialia*, vol. 45, pp. 773-779.

Yamaguchi A., Nasu S., Tanigawa H., Ono T., Miyake K., Mibu K. and Shinjo T. 2005, "Effect of Joule heating in current-driven domain wall motion", *Applied Physicsc Letters*, vol. 86, pp. 012511-1-01251-3.

Yang F., Wolke J. G. C. and Jansen J. A. 2008, "Biomimetic calcium phosphate coating on electrospun poly (ε-caprolactone) scaffolds for bone tissue engineering", *Porous Inorganic Materials for Biomedical Applications*, vol. 137, pp. 154-161.

Yashimoto H., Shin Y. M., Terai H. and Vacanti J.P. 2003, "A biodegradable nanofiber scaffold by electrospinning and its potential for bone tissue engineering", *Biomaterials*, vol. 24, pp. 2077-2082.

Yin Y., Ye F., Cui J., Zhang F., Li X. and Yao K. 2003, "Preparation and characterization of macroporous chitosan-gelatin/β-tricalcium phosphate composite scaffolds for bone tissue engineering", *Wiley Periodicals*,Inc, pp.845-855.

Yoon, D. M. and Fisher, J. P. 2006, "Polymeric Scaffolds for Tissue Engineering Applications," in The Biomedical Engineering Handbook: *Tissue Engineering & Artificial Organs*, 3 edn,

Yoshizawa S., Fourmy D. and Puglisi J. D. 1998, "Structure origins of gentamicin antibiotic action", *The EMBO Journal*, vol. 17, pp. 6437-6448.

Zaitsev V. S., Filimonov D. S., Presnyakov I. A., Gambino R. J. and Chu B. 1999, "Physical and chemical properties of magnetite and magnetite-polymer nanoparticles and their colloidal dispersions", *J. Colloid Interface Sci*. vol. 212, pp. 49-57.

Zalipsky S. 1995, "Functionalized Poly(ethy1ene glycol) for Preparation of Biologically Relevant Conjugates", *Bioconjugafe Che*, vol. 6, pp. 150-1 65.

Zambaux M. F., Bonneaux F. and Gref F. 1998, "Influence of experimental parameters on the characteristics of poly (lactic acid) nanoparticles prepared by a double emulsion method", *J. Controlled Release*, vol. 50, pp. 31-40.

Zhang J. and Misra R. D. K. 2007, "Magnetic drug-targeting carrier encapsulated with thermosensitive smart polymer: core-shell nanoparticle carrier and drug release response", *Acta Biomaterialia*, vol. 3, pp. 838-850.

Zhang Y., Kohler N. and Zhang M. 2002, "Surface modification of superparamagnetic magnetite nanoparticles and their intracellular uptake", *Biomaterials*, vol. 23, pp. 1553–1561.

Zhao M., Beauregard D. A., Loizou L., Davletov B. and Brindle K. M. 2001, "Non-invasive detection of apoptosis using magnetic resonance imaging and a targeted contrast agent", *Nat Med*, vol. 7, pp. 1241-1244.